ELSEVIER

Polymer 42 (2001) 8779–8785

polymer

www.elsevier.com/locate/polymer

Effects of solvent treatment on glass transition characteristics of treated poly(*p*-phenylene sulphide)

E. El Shafee

Department of Chemistry, Faculty of Science, Cairo University, Giza 12613, Egypt

Received 23 January 2001; received in revised form 4 May 2001; accepted 11 May 2001

Abstract

The relationship between solvent-crystallized morphology and glass transition characteristics of poly(*p*-phenylene sulphide) that had been previously processed with 1-chloronaphthalene is reported. Dielectric relaxation studies revealed a strong positive offset in glass transition temperature (T_g) of the solvent-crystallized samples compared to the corresponding amorphous sample, as well as thermally crystallized samples of similar bulk crystallinity. Additionally, the apparent activation energy for the α-relaxation was higher for the solvent-crystallized case. The dielectric relaxation strength ($\Delta\varepsilon = \varepsilon_0 - \varepsilon_\infty$) determined for the solvent-crystallized PPS is small and showing weak temperature dependence, leading to an increase in $\Delta\varepsilon$ as the temperature increased above T_g. This was explained by the existence of a large amount of tightly bound, or rigid-amorphous materials in the solvent-treated sample. We suggested that the large amount of immobile amorphous material, and its ability to relax at temperatures above T_g, is related to strong secondary crystallization process in solvent-treated PPS.

Keywords: Poly(*p*-phenylene sulphide); Solvent crystallized; Dielectric relaxation

1. Introduction

Poly(phenylene sulphide) (PPS) is a semicrystalline high performance thermoplastics with outstanding thermal and mechanical properties. PPS is finding extensive use in modern technological applications such as electronic component encapsulates, conducting polymers, printed circuit board, optical fibers, etc. [1,2]. For these applications PPS may, in some cases, be processed from solution. For example, during prepregging (e.g. in manufacturing of fiber prepregs), solvent dissolution (to lower viscosity), and final removal commonly become an essential part of processing. Although PPS has been reported to show exceptional chemical resistance and is insoluble in most common solvents, Padden and Lovinger [3] however, have shown that PPS could be successfully dissolved in 1-chloronaphthalene at elevated temperature. Possible effects of 1-chloronaphthalene solvent treatments on PPS crystallization kinetics have been reported recently [4].

The solvent-induced crystallization phenomena have been well studied in many systems by various researchers [5–7]. It was known that in the presence of certain interactive liquids, crystallization of the amorphous polymer could take place at temperatures well below the glass transition (T_g) of the polymer. The interaction of the polymer with the solvent lower the effective T_g of the material, and the polymer chains will arrange themselves onto a lower free energy state. In practice, solvent-induced crystallization is achieved via a sorption behavior.

The influence of crystalline morphology on the glass–rubber relaxation characteristics of PPS has been examined in detail [8–12]. The presence of crystallinity leads to the constraint of amorphous chain mobility in the vicinity of the glass transition. This is manifested by a positive offset of the order of 10–20°C in the glass transition of the crystalline polymer as compared to their wholly amorphous counterparts, as well as a broadening of the glass transition. For a semicrystalline PPS sample, the measured glass transition temperature is observed to decrease with less-restrictive crystalline conditions. Cold crystallization at progressively higher temperature, for example, leads to a systematic decrease in T_g, although the glass transition for all crystallized samples is still well above that measured for quenched material. This trend demonstrates that the degree of constraint imposed by the crystallites on the amorphous-phase motions is a sensitive function of crystallization history and the corresponding morphology that develops. Crystallization at conditions of relatively high chain mobility and low nucleation density leads to a morphology that imposes less constraint on the motion of the amorphous chains. This loosening of the crystalline constraint has been attributed to improved crystal perfection, i.e. a decrease in lamellar surface roughness [9].

0032-3861/01/$ - see front matter
PII: S0032-3861(01)00350-0

Table 1
Weight fraction crystallinity (X_c) and glass transition temperatures of the various PPS samples. T_g^{DSC}: glass transition; T_g^{diel}: glass transition based on the maximum loss at 1 kHz

Thermal history	X_c	T_g^{DSC} (°C)	T_g^{diel} (°C)
Amorphous	–	84	94
Solvent crystallized	0.29		148
Solvent crystallized, annealed at 200°C	0.34	105	130
Melt crystallized at 200°C	0.40	100	120
Cold crystallized at 200°C	0.38	103	123

Although these studies explore a wide range of thermal histories, back bone structure and corresponding semicrystalline morphologies, they are limited in that the possible influence of solvent-induced crystallinity is not addressed.

In the work reported here, the relationship between solvent-crystallized morphology and glass transition characteristics of PPS is examined. Solvent-induced crystallinity is expected to have a marked influence on the dynamics of the glass–rubber (α) relaxation, when compared to the corresponding amorphous sample, as well as thermally crystallized specimens.

2. Experimental

2.1. Materials and preparations

PPS was obtained from Polyscience, in a fine powder form; melt viscosity was 90 Pa s and M_n was 15,000 g/mol. The powder was Soxhlet extracted in tetrahydrofuran (THF) for 24 h to remove low molecular weight oligomers.

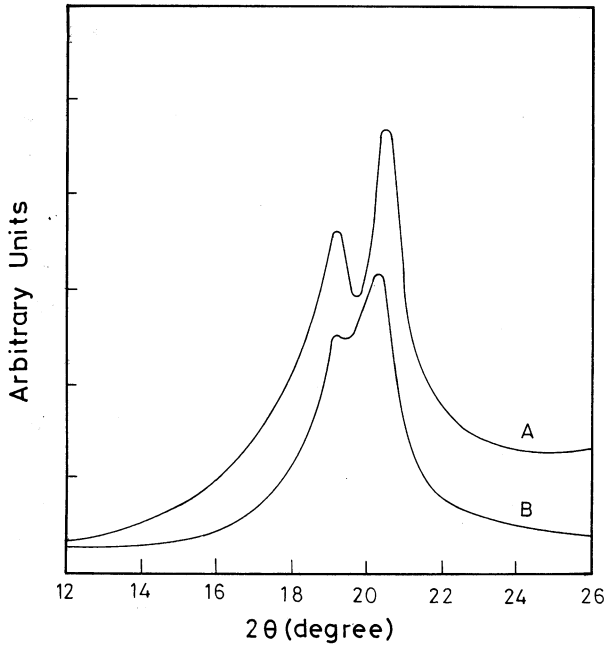

Fig. 1. WAXS pattern of (a) solvent-crystallized PPS and (b) cold-crystallized PPS; cold crystallization at 200°C for 1 h.

Thin sheets (1 mm in thickness) of amorphous PPS were prepared by compression molding of the PPS powder at 320°C for 4 min followed by quenching into liquid nitrogen. A short residence time in the melt was used to avoid curing reactions [13]. Four different crystallization methods were used: isothermal melt, cold crystallization, solvent-induced crystallization, and solvent crystallization followed by annealing. The melt crystallized sample was prepared by heating the PPS sheet to 320°C, holding for 2 min to destroy seed nuclei, then quickly cooling to 200°C and holding for 1 h. This time was chosen so that the material was fully crystalline, according to the crystallization kinetics curve determined previously [14]. The cold crystallized sample was obtained by isothermal annealing of the amorphous sheet at 200°C; crystallization time was 1 h. The solvent-crystallized specimens were prepared by immersion of the amorphous sheet in 1-chloronaphthalene at 100°C for ~60 h. The solvent-crystallized sheets were allowed to dry at ambient conditions and were then placed in a vacuum oven at 100°C until the solvent was completely extracted and dried to ensure no residual solvent left prior to use. Annealing of the solvent-crystallized material was conducted in a controlled oven at 200°C for 2 h.

The complex dielectric permittivity, ε^*, was measured using a Polymer Laboratories thermal analyzer (PL-DETA) system which consists of a General Radio 1689 M Digital precision RLC Digibridge interfaced with the Polymer Laboratories temperature controller. Concentric silver electrodes (33 mm) were vacuum evaporated directly on the samples, which were mounted between polished platens in temperature-controlled test oven. The real and the loss components of the complex dielectric permittivity were recorded at frequencies ranging from 0.1 to 100 kHz across a temperature range of 0–120°C; the heating rate was 1°C/min.

Calorimetric studies were performed using a differential scanning calorimeter (PL-DSC) of Polymer Laboratories. Indium was used as the temperature calibrator, and sapphire standard was used for the calibration of heat capacity. All scans were carried out at a scanning rate of 20°C/min under inert nitrogen.

The wide-angle X-ray diffraction (WAXD) data were obtained with a rotating-anode X-ray generator (Rigaku Denki, Rotaflex RT-300 RC) operated at 40 kV and 100 mA. The X-ray source was monochromatized to Cu Kα ($\lambda = 1.54$ Å) radiation. The WAXD pattern was taken with a fine focused X-ray source using a flat camera (Rigaku Denki, RU-100).

3. Results and discussion

Wide-angle X-ray scattering (WAXS) was used in order to obtain unambiguous, room-temperature determinations of the degree of crystallinity (X_c) in the various semicrystalline specimens. These measurements not only provide

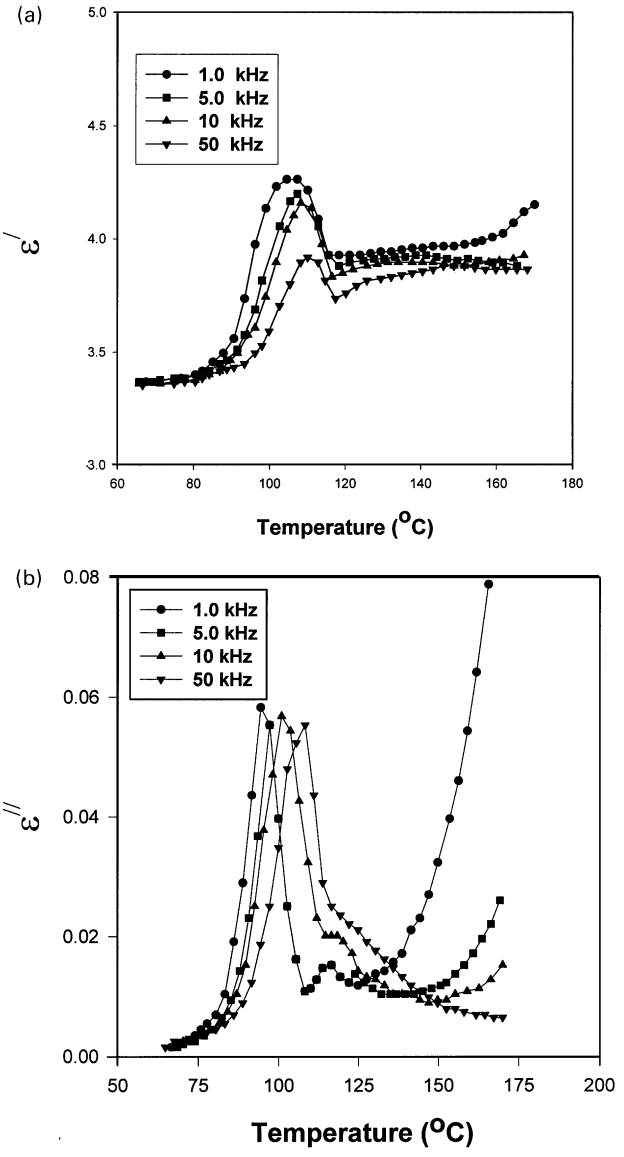

Fig. 2. Isochron showing (a) the real part, ε', and (b) the imaginary part, ε'' of the complex permittivity as a function of temperature for amorphous PPS at various frequencies.

reliable values of X_c, but offer additional insight as solvent-induced residual crystals in PPS. The crystallinity of the samples was calculated using Vonk's method [15] by subtracting the background and curve fitting the amorphous contribution to the peak crystalline intensities and using relative integrated areas for calculation. The values of X_c for various PPS samples are reported in Table 1. For the crystallization histories considered here, the highest crystallinity was obtained for both cold-crystallized and melt-crystallized PPS. The degree of the crystallinity in solvent-crystallized sample is lower than that of the thermally crystallized PPS. Annealing of the solvent-crystallized samples at 200°C, for example, leads to a small increase in the crystallinity index.

In Fig. 1, the WAXS profiles of thermally crystallized and solvent-crystallized PPS are presented. No new peaks appear in the diffraction pattern of the solvent-crystallized PPS thereby suggesting that this specimen has the same crystalline unit cell as the thermally crystallized samples. The solvent thus serves only as a plasticizing agent. However, the WAXS patterns of thermally crystallized samples exhibit relatively narrow peaks, which are indicative of large crystals, while the solvent-crystallized samples exhibit relatively broad peak indicating small crystals.

The glass transition temperatures of the amorphous and the crystallized PPS samples as determined by DSC are listed in Table 1. Examination of the results for crystallized PPS reveals a significant positive offset in glass transition temperature compared to the wholly amorphous quenched sample. These data are fully consistent with data reported previously for PPS [8,10] and for other semiflexible, low crystalline homopolymers such as poly(ethylene terephthalate) (PET) [16] and poly(ether ether ketone) (PEEK) [17,18]. This offset in T_g reflects the constraint imposed on the amorphous segment motions by the crystallites. The solvent-crystallized sample does not present a clear T_g step when scanned calorimetrically. However, the annealed solvent-crystallized specimens showed a discernible T_g that are higher than those measured for samples prepared either by melt or cold crystallization. This indicates a sizable degree of constraint that persists from the crystalline surfaces into the amorphous phase.

Dielectric relaxation results for amorphous PPS in the vicinity of the glass–rubber relaxation are plotted isochronally as real dielectric permittivity (ε') and dielectric loss (ε'') versus temperature in Fig. 2. Examination of the dielectric constant shows a strong, stepwise increase in ε' starting at $\cong$ 100°C, which corresponds to large-scale mobilization of the amorphous chain, i.e. the glass–rubber relaxation; this is accompanied by a narrow peak in dielectric loss. The abrupt, frequency-independent decrease in dielectric permittivity that is observed at $\approx$ 130°C corresponds to the onset of the cold crystallization in the non-isothermal scan, as some fraction of the responding dipoles are immobilized by the evolving crystalline structure. The presence of crystallinity leads to a broadening of the α-relaxation, and the eventual mobilization of the remaining amorphous material at high temperature (>130°C) is evident as a gradual increase in ε' and a broad shoulder on the high temperature side of the glass transition loss peak.

Dielectric data for solvent-crystallized PPS sample is shown in Fig. 3. In this case, a single incremental increase in dielectric permittivity is observed at the glass transition, which is not complicated by the effect of the crystallization during the scan. The dielectric loss peak for the solvent-crystallized sample is considerably broadened as compared to wholly amorphous specimen, as the responding chains experience a much wider spectrum of local relaxation environments. This explains why this material does not show a clear T_g step when subjected to DSC scan. In calorimetric measurements, a scan rate of 20°C/min

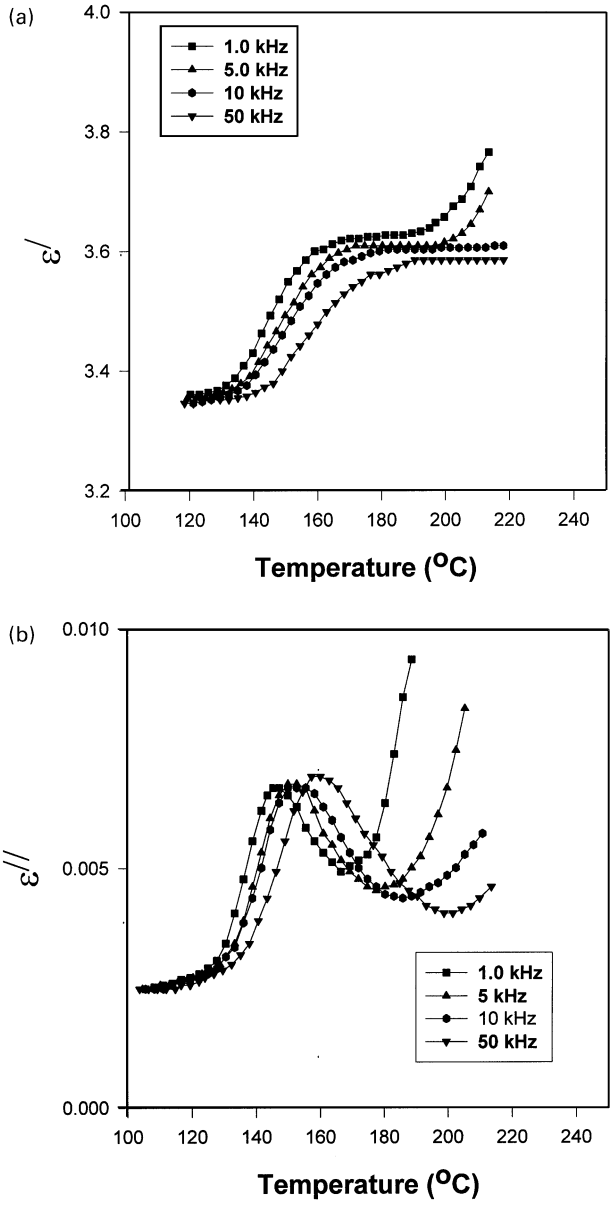

Fig. 3. Isochron showing (a) the real part, ε', and (b) the imaginary part, ε'', of the complex permittivity as a function of temperature for solvent-crystallized at various frequencies.

constitutes a very low effective frequency [19,20] and the amorphous phase can relax little by little throughout the scan. However, in the dielectric experiments which is performed at much higher frequency, the solvent-crystallized samples present a clear dielectric T_g at ~145°C (1 kHz).

Dielectric glass transition temperature (T_g^{diel}, 1 kHz) based on the maximum in the dielectric loss are reported for the amorphous and crystallized PPS samples in Table 1. The large offset in the glass transition temperature is observed for the solvent-crystallized sample. The dielectric glass transition for PPS samples recrystallized (i.e. solvent crystallized then annealed at 200°C) is intermediate to the

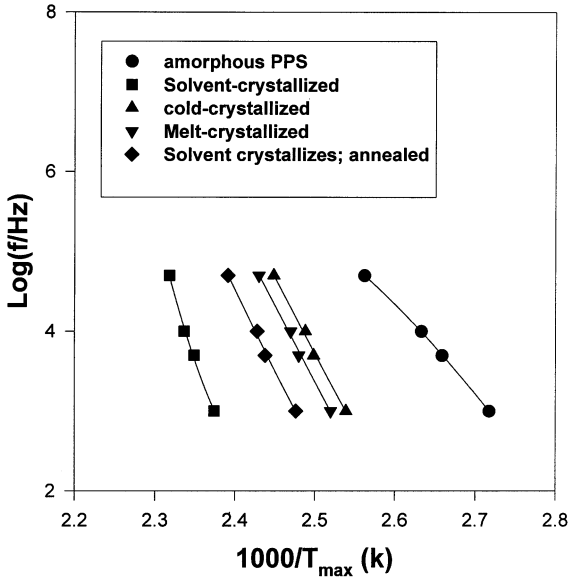

Fig. 4. Arrhenius plots of dielectric test frequency (Hz) versus $1000/T_m$ (K) for amorphous and different crystallized PPS samples.

values obtained for the solvent-crystallized samples and samples prepared by direct cold or melt crystallization. This indicates reorganization leading to a loosening of the crystalline constraint imposed on the amorphous phase. It might be added that the trends observed in the dielectric data are consistent with calorimetric studies, although a stronger positive offset in transition temperature with the presence of crystallinity is observed for the dielectric results. This behavior suggests that the dielectric probe is somewhat more sensitive to the constraining influence of crystallinity in these samples as compared to calorimetric measurements.

The time–temperature characteristics of the α-relaxation are plotted in an Arrhenius manner for the amorphous and the crystallized PPS samples in Fig. 4; these data are based on the maximum in the isochronal dielectric loss curves for the various samples. Each data set can be satisfactorily described using a WLF (Williams–Landel–Ferry) expression across the range of frequency examined [21]. The results demonstrate the relative displacement in glass–rubber relaxation temperature for solvent-crystallized samples relative to the quenched amorphous material, with the location of the recrystallized samples data situated in between the data of thermally crystallized and solvent-crystallized sample. The local slope of the Arrhenius curves is higher for the solvent-crystallized as compared to thermally crystallized case, which is consistent with a higher apparent activation energy for the glass–rubber relaxation in solvent-crystallized materials.

The marked variation in relaxation temperature and apparent activation energy for solvent-crystallized sample as compared to thermally crystallized samples indicates that the solvent crystallization results in a morphological fine structure of significantly different character. Indeed, our WAXS results (Fig. 1) indicate a broader diffraction peak

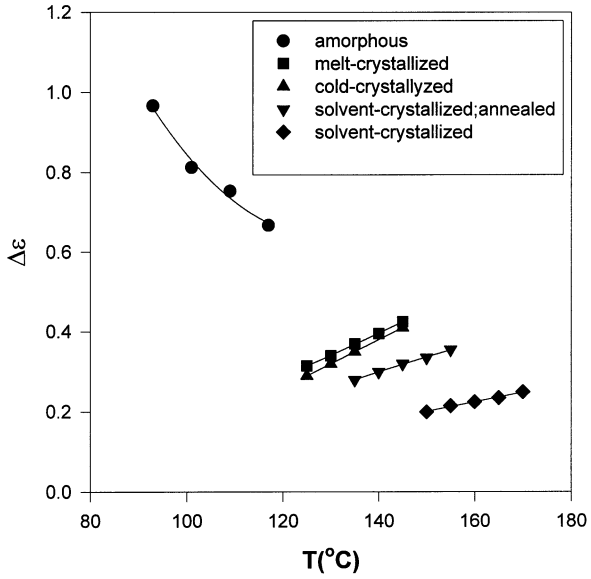

Fig. 5. Dielectric relaxation strength, $\Delta\varepsilon$, versus temperature for amorphous and crystallized PPS samples.

(i.e. larger full width at half maximum) for solvent-crystallized specimen relative to that observed for thermally crystallized one. This suggests the presence of tinier crystallites in solvent-crystallized material, with the crystallites imposing a much stronger degree of constraint on the relaxing amorphous segments. This leads to an overall increase in the central relaxation time as well as an increase in activation energy associated with long-range chain.

Crystallization kinetics studies [4] show that when PPS is isothermally cold crystallized, the kinetics can be described nearly by a single Avrami exponent over the entire crystallization period. This indicates that there is only one process governing crystallization (the 'primary' crystallization) and this persists until crystallization is complete. On the other hand, for solvent-treated PPS, the Avrami crystallization plot appeared as two straight portions with an apparent discontinuity [4]. The causes for the differences were related to sequential development of two types of crystalline entities. This means that in a solvent-crystallized sample, a large fraction of thinner lamellar branches develops, located in between the dominant lamellae or as imperfect interspherulite crystal-like micelles highly impinged by the growing front of spherulites. These subsidiary crystals may serve to interrupt and hence constrain the amorphous phase, creating a large fraction of tightly bound or, rigid-amorphous material.

It is well known that the motions of chains in the vicinity of crystalline regions are highly constrained compared with similar motions in fully amorphous phase [22,23]. In addition to general chain constraint, the existence of a 'rigid-amorphous phase' (RAP) has been postulated to exist in a number of semicrystalline polymers [8–10,18], including PPS, where those amorphous chains which are in close proximity to crystalline regions are constrained and are only able to relax at temperatures above the glass transition. Experimental investigations of PAP in PPS have been carried out using DSC [8,9] and dielectric relaxation spectroscopy [10]. The essential parameter for quantifying the RAP in dielectric relaxation measurements is the dielectric relaxation strength or increment ($\Delta\varepsilon = \varepsilon_0 - \varepsilon_\infty$). This method involves a comparison of $\Delta\varepsilon$ of amorphous and isothermally crystallized samples as a function of temperature to demonstrate that increasing numbers of dipoles only begin to relax above the normal glass temperature, as the RAP becomes mobile. The strength of a particular relaxation process can be established from the fitting of common empirical relaxation functions to dielectric data measured in the frequency domain, usually represented in the form of Cole–Cole or loss/frequency plots.

For the PPS samples investigated here, the relaxation was symmetric and was described by the Cole–Cole function [24]. We therefore chose to fit our data using the minimum number of adjustable parameters, by fitting to a circle with origin displaced below the $\varepsilon'' = 0$ line [25]. Non-linear least-squares curve fitting using a Marquardt least-squares algorithm [25] was performed to find γ, ε_0 and ε_∞.

The temperature dependence of $\Delta\varepsilon$ in the vicinity of the glass transition for the amorphous and various crystallized PPS samples are shown in Fig. 5. The dielectric relaxation strength for the amorphous sample above T_g is strongly temperature dependent, with $\Delta\varepsilon$ decreasing with increasing temperature in accord with a simple Onsager model of dipolar orientational effects. The amorphous-phase relaxation in the semicrystalline samples had a completely different temperature dependence, leading to an increase in dielectric relaxation strength as the temperature increased above T_g. This increase in $\Delta\varepsilon$ has been attributed to the progressive mobilization of 'rigid-amorphous' material in the vicinity of the crystal-amorphous interphase which relaxes gradually above the T_g of the mobile-amorphous fraction [10,12,18].

An interesting special case is provided by the solvent-crystallized PPS sample. This specimen showed the smallest relaxation strength and the weaker temperature dependence of $\Delta\varepsilon$. Also, this sample has a relatively low degree of crystallinity (see Table 1). These results indicate a high fraction of RAP in the solvent-crystallized material.

In order to quantify the relative population of the amorphous-phase dipoles, which participate in the glass–rubber relaxation at a given temperature, the dielectric mobile-amorphous-phase fraction is defined as [10,18]:

$$\beta(T) = \frac{\Delta\varepsilon(T)^{sc}}{\Delta\varepsilon(T)^{a}} \tag{1}$$

where $\Delta\varepsilon^{sc}(T)$ is the measured relaxation intensity of the semicrystalline sample and $\Delta\varepsilon^{a}(T)$ the relaxation intensity of the wholly amorphous specimen evaluated at the same temperature. Here, the definition of $\beta(T)$ is valid at temperature $T > T_g$. For temperature $T < T_g$, $\beta(T)$ is zero. This expression is completely analogous to the definition of mobile-amorphous-phase fraction based on

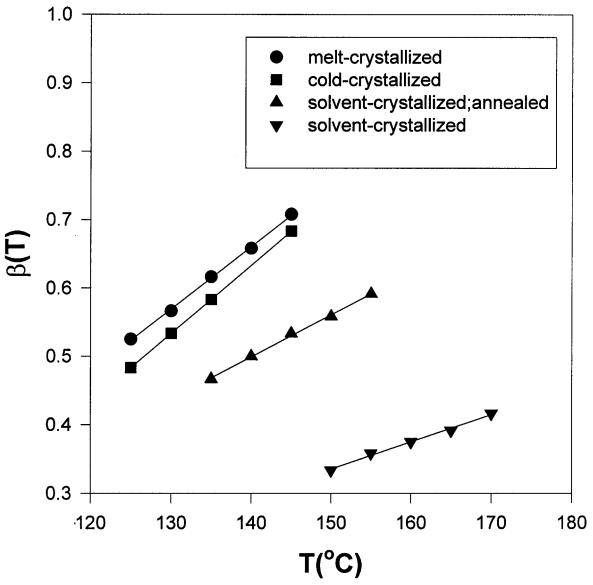

Fig. 6. The parameter, $\beta(T)$, versus temperature for the crystallized PPS samples.

normalized increase in heat capacity. In Eq. (1), the parameter of $\beta(T)$ indicates all the mobile-amorphous-phase fraction obtained from the heat capacity increment and possibly some fraction of the rigid-amorphous phase that is relaxed at $T > T_g$ but considered rigid at the calorimetric glass transition (i.e. T_g^{DSC}). The dielectric relaxation method [10,18] has a distinct advantage over the use of heat capacity [8,9] to determine the fraction of the mobile phase. This is because the amount of rigid-amorphous-phase material, ϕ_{RAP}, can be found directly from the knowledge of $\beta(T)$ and does not require any prior measurements of the degree of crystallinity. Extrapolation of $\beta(T)$ to the T_g of the semicrystalline sample gives the initial amount of mobile-amorphous-phase fraction (ϕ_{MA}) (which can be found from heat capacity increment), while extrapolation of $\beta(T)$ to T_m gives the total amount of the mobile-amorphous phase plus RAP (i.e. $\phi_{MA} + \phi_{RAP}$) [10,18]. The amount of RAP material is then found from

$$\phi_{RAP} = \beta(T_g \leq T \leq T_m) - \phi_{MA} \quad (2)$$

The values of $\beta(T)$, as calculated from Eq. (1) (taken the value of $\Delta\varepsilon^a = 0.6$, independent of temperature) for the different crystallized samples are plotted versus temperature in Fig. 6. Comparison of the values of the dielectric mobile fraction ($\beta(T) = \Delta\varepsilon^{sc}/\Delta\varepsilon^a$) with the degree of crystallinity present in these samples (see Table 1) shows that the amorphous phase is not fully mobilized across this temperature range. Thus, the increase in the mobile-amorphous fraction that is observed with temperature is most likely due to progressive mobilization of the RAP, as has been reported previously [8,10,12]. The observed increment in the RAP fraction for the solvent-crystallized sample as compared to other thermally crystallized samples (as deduced by the decrease of the dielectric relaxation strength of the mobile fraction) could be interpreted as due the formation of small, imperfect crystals as a result of secondary crystallization. Formation of secondary crystals is thought to occur between dominant lamellae leading to a large roughness of the interfaces. This would enhance the interaction between the amorphous and the crystal phases and consequently make the mobile-amorphous phase couple more tightly with the RAP. Other experiments need to be done in order to confirm our suggestion that the interface roughness in solvent-treated PPS is the important factor to determine the glass transition characteristics of PPS.

4. Conclusion

The dielectric relaxation characteristics of solvent-crystallized PPS have been investigated in the region of the glass–rubber (α) relaxation. Solvent-induced crystallinity has a marked influence in the glass transition temperature of the material, with T_g offset well above the glass transition temperature for thermally crystallized PPS materials. Annealing of the solvent-crystallized sample leads to a change in morphology such that the offset in T_g is reduced. The apparent activation energy for the α-relaxation was higher for the solvent-crystallized case. With regard to dielectric relaxation strength, both thermally and solvent-crystallized PPS show an increase of $\Delta\varepsilon$ with temperature. In the solvent-crystallized case, the temperature dependence of $\Delta\varepsilon$ was less remarkable, indicating a large fraction of immobile amorphous material. These results are consistent with the evolution of a tighter crystalline morphology in solvent-crystallized specimen as compared to thermally crystallized samples, with the crystallites imposing a much stronger degree of constraint on the relaxing amorphous segments. Our X-ray data confirm these findings.

References

[1] Kelleher PG, Hubbaur P. In: Proceedings of the 36th ANTEC, SPE; 1978. p. 340.
[2] Clarke TC, Kanazawa KK, Lee VY, Rabolt JF, Reynolds JR, Street GB. J Polym Sci, Phys Ed 1982;20:117.
[3] Padden FJ, Lovinger AJ. Bull Am Phys Soc 1982;27:259.
[4] Woo EM, Chen JM. J Polym Sci, Phys Ed 1995;33:1985.
[5] Wolf CJ, Barnmann JA, Grayson MA, Anderson DP. J Polym Sci, Phys Ed 1992;30:251.
[6] Khanna YP, Kumar R, Reimschuessel AC. Polym Engng Sci 1988;28:1612.
[7] Muellerleile JT, Freeman JJ. J Appl Polym Sci 1994;54:135.
[8] Cheng SZD, Wu ZQ, Wunderlish B. Macromolecules 1987;20:2802.
[9] Huo P, Cebe P. Colloid Polym Sci 1992;270:840.
[10] Huo P, Cebe P. J Polym Sci, Phys Ed 1992;30:239.
[11] Wu SS, Kalika DS, Lamonte RR, Makhija S. J Macromol Sci, Phys Ed B 1996;35:157.
[12] Kalika DS, Wu SS, Lamonte RR, Makhija S. J Macromol Sci, Phys Ed B 1996;35:179.
[13] Lpez LC, Wilkes GL. Polymer 1988;29:106.
[14] Chung JS, Cebe P. J Polym Sci, Phys Ed 1992;33:163.

[15] Vonk CG. J Appl Crystallogr 1973;6:148.
[16] Schlosser E, Schonhals A. Colloid Polym Sci 1989;267:963.
[17] Cheng SZQ, Cao MY, Wunderlich B. Macromolecules 1986;19:1868.
[18] Huo P, Cebe P. Macromolecules 1992;25:902.
[19] Donth E. J Non-Cryst Solids 1982;53:325.
[20] Schick C, Nedbal J. Prog Colloid Polym Sci 1988;78:9.
[21] Ferry JD. Viscoelastic properties of polymers. New York: Wiley, 1980.
[22] Williams G. Adv Polym Sci 1979;33:59.
[23] Fzquerra TA, Balta-Calleja FJ, Zachmann HG. Polymer 1994;35:2600.
[24] Cole RH, Cole KS. J Chem Phys 1941;9:341.
[25] Bevington PR. Data reduction and error analysis for physical science. New York: McGraw-Hill, 1969.